Bol. Soc. Paran. Mat.
©SPM – E-ISSN-2175-1188
SPM: www.spm.uem.br/bspm

(3s.) **v. 2026 (44) 2** : 1–20.
ISSN-0037-8712
doi:10.5269/bspm.78969

Numerical Approaches to HIV/AIDS Dynamics: A SIAT Model Study

Kshama Jain, Anuradha Bhattacharjee, Srikumar K.

ABSTRACT: In this study, we develop and analyze a nonlinear $SIAT$ model to investigate the transmission dynamics of HIV/AIDS with an emphasis on the role of treatment. The total population is stratified into four compartments: Susceptible (S), Infected (I), individuals with AIDS (A) and Treated (T). The model's equilibriums are derived, and the basic reproduction number R_0 is calculated as the threshold parameter governing disease persistence or eradication. Both local and global stability conditions of the equilibriums are rigorously established. A sensitivity analysis of R_0 identifies the parameters most influential in driving HIV/AIDS progression, providing valuable insights for potential intervention strategies. To complement the theoretical analysis, three numerical schemes—Euler's method, the fourth-order Runge–Kutta method, and the forward difference method—are employed to simulate system dynamics. A comparative evaluation highlights their relative accuracy and efficiency in capturing the model's behavior. Numerical experiments, conducted using MATLAB, illustrate the impact of treatment and validate the analytical results.

Key Words: HIV/AIDS dynamics, $SIAT$ model, basic reproduction number, sensitivity analysis, numerical methods, treatment effect.

Contents

1. Introduction

HIV/AIDS remains a significant global public health issue, affecting millions of people worldwide despite decades of medical progress and preventive initiatives. Over the last fifty years, the epidemic has continued to expand, with new infections and AIDS related deaths still occurring each year. According to the World Health Organization (WHO), approximately 39 million people were living with HIV in 2023, and about 630,000 individuals died due to AIDS-related illnesses [1]. Although substantial advancements have been

2010 *Mathematics Subject Classification:* 92D30, 34A34, 65L06.

Submitted September 24, 2025. Published December 19, 2025

made in Antiretroviral Therapy (ART)and other public health measures, the disease continues to spread, largely due to diverse transmission modes and underlying socioeconomic challenges.

HIV is primarily transmitted through unprotected sexual contact, reuse of infected needles and practices like tattooing and body piercing with contaminated instruments. Once inside the body, the virus targets $CD4^+$ T-cells (the critical components of the immune system that help fight infections), HIV integrates its genetic material into the host DNA, allowing it to replicate and progressively deplete these immune cells, which over time compromises the immune system [2]. In the early phase, individuals may experience mild flu-like symptoms, which typically subside as the infection enters a latent stage. Without timely detection and treatment, the immune system deteriorates further, potentially leading to Acquired Immunodeficiency Syndrome (AIDS) within approximately 4–5 years [3]. The primary method for managing HIV infection is Antiretroviral Therapy (ART), which suppresses viral replication, reduces viral load and slows disease progression. When consistently adhered to, ART significantly enhances the quality of life for people living with HIV and delays the progression to AIDS. However, ART is not a cure; it controls the infection rather than eliminating it. Interruptions in treatment or poor adherence can lead to drug resistance, reducing treatment efficacy and increasing the risk of disease progression [4]. The success of ART also depends on factors such as medication availability, patient adherence and access to healthcare services. Socioeconomic barriers, stigma and inequalities in healthcare access continue to hinder effective treatment, thereby perpetuating the epidemic [5].

Mathematical modeling has been instrumental in understanding the transmission dynamics of HIV/AIDS and evaluating the impact of interventions. Early models, such as those proposed by Anderson and May (1987), employed SIS and SIR frameworks to study disease spread [6]. Since then, numerous researchers have refined these models to incorporate additional epidemiological factors, including awareness levels, co-infections and treatment dynamics. For instance, some models differentiate between aware and unaware infected individuals [7], while others explore the effects of ART and the emergence of drug resistance [8]. Advanced numerical methods have been employed to analyze these models, offering insights into effective disease control strategies.

Waziri et al. [9] examined HIV/AIDS dynamics incorporating vertical transmission and treatment using the SIPTA model (Susceptible, Infected, Pre-AIDS, Treated, AIDS). Ming Wan Shen et al. [10] developed an age-structured model to track infection transmission and estimate patient longevity based on ART initiation timing. David Fajardo-Ortiz et al.'s [11] research is shaped not only by the division of the problem into specific components and interactions, resulting in increasingly specialized research communities, but also by shifts in the technological landscape and the significant epidemiological changes that took place between 1993 and 1995. Attaullah et al.'s [12] study discuss and analyze the effect of constant and different variable source terms (depending on the viral load) used for the supply of new $CD4^+$ T-cells from thymus on the dynamics of $CD4^+$ T-cells, infected $CD4^+$ T-cells and free HIV virus. Haoran Sun et al. [13] proposed a computational method to accurately estimate the number of infectious individuals during Taiwan's early surveillance phase (January 2005 to December 2006), using a compartmental model named SIAJB (Susceptible, Infectious HIV, Non-Infectious HIV, Infectious AIDS, Non-Infectious AIDS). Morani et al. [14] introduced the SWIUA model (Susceptible, Untested, Transmittable Virus Infected, Untransmittable Virus Infected, AIDS), which accounted for both symptomatic and asymptomatic individuals.

To effectively analyze the complex disease dynamics captured by the mathematical model, numerical methods serve as important techniques for obtaining approximate solutions and exploring the system's behavior under various conditions. Numerous researchers have compared different numerical approaches to determine their accuracy and suitability in solving such infectious disease models. Rizki Ashgi et al. [15] studied the infectious diseases Covid-19 by using the SIR model to solve the system. They used two numerical methods, namely Euler Method and 4th order Runge–Kutta. In the paper, they study the performance and comparison of both methods in solving the model. Aakash M et al. [16] studied infectious diseases to solve the mathematical model using some numerical methods, by transforming the equations into the Euler and Runge–Kutta methods. They did not only study the comparison of these two methods, also found out the differences in solutions between the two methods. However, there remains limited work that systematically examines the relative performance of multiple numerical approaches in

the context of HIV/AIDS dynamics, particularly when treatment effects are explicitly included.

To address this gap, we develop a nonlinear compartmental model—SIAT (Susceptible–HIV Infected–AIDS–Treated) to examine the progression of HIV/AIDS and perform an analytical analysis of the study. The study also assesses the performance of three numerical techniques: Euler's method, the 4th-order Runge–Kutta method and the Forward Difference method. The aim is to evaluate the accuracy, stability and computational efficiency of these methods in simulating disease progression. Through this combined analytical–numerical approach, we seek to establish a reliable computational framework to better understand disease dynamics and enhance intervention strategies.

This study is organized as follows: Section 2 outlines the formulas for the three numerical methods used in analyzing the model. Section 3 presents the formulation of the HIV/AIDS model, including the determination of equilibrium points and an analysis of their global stability. Section 4 is dedicated to sensitivity analysis. Section 5 defines and studies optimal control. Section 6 focuses on the numerical results, presenting simulation outcomes and comparing the absolute differences across the three numerical methods. Section 7 summarizes the study's findings.

2. Methods: Euler, 4th order Runge–Kutta and Forward Difference

To numerically solve the proposed model, we employ three widely used methods: Euler's method, the 4th order Runge–Kutta (RK4) method, and the Forward Difference (Explicit Euler) method. While the Euler method is simple and computationally efficient, it tends to accumulate errors over time, leading to significant deviations in long-term simulations. The RK4 method, known for its fourth-order accuracy and ability to handle stiff systems, is considered a benchmark in epidemiological modeling due to its high precision [16]. The Forward Difference method is also straightforward to implement but can suffer from numerical instability unless very small step sizes are used.

In all three methods, the dependent variable y is computed iteratively as the independent variable x increases in uniform small steps [17].

The Euler method can generally be expressed as follows:

$$y_{n+1} = y_n + h\, f\,(x_n, y_n)\,, \quad n = 0, 1, 2, \ldots .$$

For the fourth order Runge–Kutta method, we have

$$y_{n+1} = y_n + \frac{1}{6}\,(k_1 + 2k_2 + 2k_3 + k_4)\,,$$

where

$$k_1 = h\, f(t_n, y_n), \qquad k_2 = h\, f\left(t_n + \frac{1}{2}h, y_n + \frac{1}{2}k_1\right),$$

$$k_3 = h\, f\left(t_n + \frac{1}{2}h, y_n + \frac{1}{2}k_2\right), \qquad k_4 = h\, f\,(t_n + h, y_n + k_3)\,.$$

In the Forward Difference method, we have

$$p = \frac{x - x_0}{h},$$

$$y_n(x) = y_0 + p\Delta y_0 + \frac{p(p-1)}{2!}\Delta^2 y_0 + \frac{p(p-1)(p-2)}{3!}\Delta^3 y_0 + \cdots ,$$

where $\Delta y_0 = y_1 - y_0$.

These numerical schemes are applied to the SIAT model, and the resulting systems are solved using MATLAB to generate simulations and compare the accuracy, stability, and efficiency of the methods.

Table 1: Description of classes and parameters.

Classes and Parameters	Description
S	Susceptible class
I	HIV infected class
A	AIDS class
T	Treated class
N	Total population
α	Rate of susceptible entering into HIV infected class
k_1	Rate of HIV infected entering into AIDS class
γ	Rate of AIDS infected entering into treated class
k_2	Rate of HIV infected entering into treated class
μ	Natural death rate
d_1	Death rate due to HIV infection
d_2	Death rate due to AIDS disease

3. Mathematical Formulation

We consider an SIAT model with four classes: Susceptible, HIV infected, AIDS, Treated. The description of the classes and the parameters is given in Table 1.

The compartment diagram for the SIAT model is presented in Fig. 1.

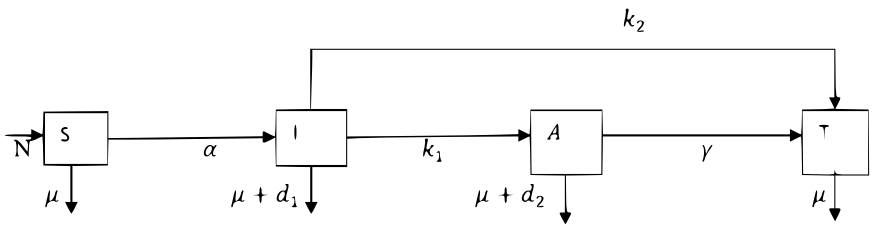

Figure 1: SIAT model.

By considering all the classes and the parameters, the HIV/AIDS model shown in Fig. 1 can be defined as

$$\frac{dS}{dt} = N - \alpha SI - \mu S, \tag{3.1}$$

$$\frac{dI}{dt} = \alpha SI - (k_1 + k_2 + \mu + d_1)\, I, \tag{3.2}$$

$$\frac{dA}{dt} = k_1 I - (\gamma + \mu + d_2)A, \tag{3.3}$$

$$\frac{dT}{dt} = k_2 I + \gamma A - \mu T. \tag{3.4}$$

The initial conditions are

$$S(0) > 0, \quad I(0) \geq 0, \quad A(0) \geq 0, \quad T(0) \geq 0.$$

3.1. Invariant region

Given the structure of the population model, it is essential to impose non-negativity constraints on all compartmental variables $S(t), I(t), A(t), T(t)$ to reflect realistic population dynamics for all $t \geq 0$. The

solution with the initial positive data stays positive for all positive t and it is bounded. It is practical to observe from the system that

$$\sup_{t\to+\infty} N(t) \leq \frac{N}{\mu}.$$

As such we can study the system in the feasible region

$$\Omega = \left\{ (S(t), I(t), A(t), T(t)) \in \mathbb{R}^4_+ : 0 \leq N(t) \leq \frac{N}{\mu} \right\}.$$

Ω is now a positive invariant set for the model. The SIAT model is epidemiologically well posed and all the solutions to the system with $(S(t), I(t), A(t), T(t)) \in \mathbb{R}^4_+$ remain in Ω.

3.2. Basic reproduction number

One important epidemiological indicator that measures the standard amount of secondary infections caused by one infectious individual in a fully susceptible population is the basic reproduction number. The next generation approach is employed for calculating the basic reproduction number [18].

Let

$$F = \begin{bmatrix} \alpha S & 0 \\ 0 & 0 \end{bmatrix}, \qquad V = \begin{bmatrix} -(k_1 + k_2 + \mu + d_1) & 0 \\ k_1 & -(\gamma + \mu + d_2) \end{bmatrix}.$$

Here F is the non-negative matrix of new infections and V is the non-singular matrix of compartmental change. We need the largest eigenvalue of FV^{-1} for the basic reproduction number. Mathematically we calculate the inverse of V:

$$V^{-1} = \frac{1}{(k_1 + k_2 + \mu + d_1)(\gamma + \mu + d_2)} \begin{bmatrix} -(\gamma + \mu + d_2) & 0 \\ -k_1 & -(k_1 + k_2 + \mu + d_1) \end{bmatrix}.$$

Multiplying F by V^{-1} we obtain

$$FV^{-1} = \frac{1}{(k_1 + k_2 + \mu + d_1)(\gamma + \mu + d_2)} \begin{bmatrix} -\alpha S(\gamma + \mu + d_2) & 0 \\ 0 & 0 \end{bmatrix}.$$

The largest eigenvalue is the basic reproduction number

$$R_0 = \frac{\alpha N}{\mu(k_1 + k_2 + \mu + d_1)}.$$

3.3. Equilibrium points

Analytical solutions to ODEs are particularly valuable, as they offer precise mathematical expressions that describe the behavior of physical systems [19]. There are two types of equilibrium: (i) disease free equilibrium, (ii) endemic equilibrium. The disease free equilibrium represents a state where no individuals in the population are infected with HIV/AIDS, while the endemic equilibrium corresponds to a persistent presence of HIV/AIDS in the population at a constant level.

3.3.1. Disease free equilibrium. For the disease free equilibrium we put $I_0 = 0$, $A_0 = 0$, $T_0 = 0$ and obtain

$$E_0 = (S_0, I_0, A_0, T_0) = \left(\frac{N}{\mu}, 0, 0, 0 \right).$$

3.3.2. Local stability of the DFE. **Theorem 1.** *The HIV/AIDS model's disease free equilibrium is locally asymptotically stable if* $R_0 < 1$.

Proof. For examining local stability we construct the Jacobian matrix at E_0:

$$J_0 = \begin{bmatrix} -\mu & -\dfrac{\alpha N}{\mu} & 0 & 0 \\ 0 & \dfrac{\alpha N}{\mu} - (k_1 + k_2 + \mu + d_1) & 0 & 0 \\ 0 & k_1 & -(\gamma + \mu + d_2) & 0 \\ 0 & k_2 & \gamma & -\mu \end{bmatrix}.$$

Its characteristic equation is $|J_0 - \lambda I| = 0$, that is

$$(\mu + \lambda)^2 \left(\frac{\alpha N}{\mu} - (k_1 + k_2 + \mu + d_1) - \lambda \right) (-(\gamma + \mu + d_2) - \lambda) = 0.$$

We get the eigenvalues

$$\lambda = -\mu, -\mu, -(\gamma + \mu + d_2), \frac{\alpha N}{\mu} - (k_1 + k_2 + \mu + d_1).$$

By the Routh–Hurwitz criterion [20], for the stability of the equilibrium, all the eigenvalues must have negative real part. This is equivalent to

$$\frac{\alpha N}{\mu} - (k_1 + k_2 + \mu + d_1) < 0,$$

namely

$$\frac{\alpha N}{\mu (k_1 + k_2 + \mu + d_1)} < 1,$$

that is $R_0 < 1$. Hence the disease free equilibrium is locally stable if $R_0 < 1$. □

3.3.3. Global stability of the DFE. **Theorem 2.** *The HIV/AIDS model's state of the system where no disease is present is globally asymptotically stable if $R_0 < 1$.*

Proof. We construct a Lyapunov function for the SIAT model as

$$V(S, I, A, T) = C_1 I + C_2 A.$$

Then

$$\frac{dV}{dt} = C_1 I' + C_2 A'.$$

Using (3.2)–(3.3), we obtain

$$\frac{dV}{dt} = C_1 \left[\alpha S - (k_1 + k_2 + \mu + d_1) \right] I + C_2 \left[k_1 I - (\gamma + \mu + d_2) A \right].$$

Using $S \leq N/\mu$ we get

$$\frac{dV}{dt} \leq C_1 \left[\alpha \frac{N}{\mu} - (k_1 + k_2 + \mu + d_1) \right] I + C_2 \left[k_1 I - (\gamma + \mu + d_2) A \right].$$

Rearranging,

$$\frac{dV}{dt} \leq \left\{ C_1 \left[\alpha \frac{N}{\mu} - (k_1 + k_2 + \mu + d_1) \right] + C_2 k_1 \right\} I - C_2 (\gamma + \mu + d_2) A.$$

Choose $C_1 = 1$ and

$$C_2 = \frac{1}{k_1} \left[-\alpha \frac{N}{\mu} + (k_1 + k_2 + \mu + d_1) \right].$$

Then

$$\frac{dV}{dt} \leq (R_0 - 1)(\gamma + \mu + d_2) \frac{(k_1 + k_2 + \mu + d_1)}{k_1} A.$$

Thus, if $R_0 < 1$ we have $\dfrac{dV}{dt} \leq 0$ with equality only when $A = 0$. Hence the disease free equilibrium is globally stable if $R_0 < 1$. □

3.4. Endemic equilibrium

Let

$$E^* = (S^*, I^*, A^*, T^*) \neq (0, 0, 0, 0)$$

be an endemic equilibrium of system (3.1)–(3.4). We solve the steady state equations.

From (3.2) we get

$$S^* = \frac{k_1 + k_2 + \mu + d_1}{\alpha} = \frac{N}{\mu R_0}.$$

Using (3.1) we obtain

$$I^* = \frac{N}{k_1 + k_2 + \mu + d_1} - \frac{\mu}{\alpha} = \frac{\alpha}{\mu} R_0 - \frac{\mu}{\alpha}.$$

From (3.3),

$$A^* = \frac{k_1}{\gamma + \mu + d_2} \left[\frac{N}{k_1 + k_2 + \mu + d_1} - \frac{\mu}{\alpha} \right] = \frac{k_1}{\gamma + \mu + d_2} \left[\frac{\alpha}{\mu} R_0 - \frac{\mu}{\alpha} \right].$$

From (3.4),

$$T^* = \frac{k_2 I^* + \gamma A^*}{\mu} = \frac{1}{\mu} \left[k_2 + \frac{\gamma k_1}{\gamma + \mu + d_2} \right] \left[\frac{\alpha}{\mu} R_0 - \frac{\mu}{\alpha} \right].$$

Therefore we can write the endemic equilibrium as

$$E^* = \left(\frac{N}{\mu R_0}, \frac{\alpha}{\mu} R_0 - \frac{\mu}{\alpha}, \frac{k_1}{\gamma + \mu + d_2} \left[\frac{\alpha}{\mu} R_0 - \frac{\mu}{\alpha} \right], \frac{1}{\mu} \left[k_2 + \frac{\gamma k_1}{\gamma + \mu + d_2} \right] \left[\frac{\alpha}{\mu} R_0 - \frac{\mu}{\alpha} \right] \right).$$

3.4.1. Local stability of the endemic equilibrium. **Theorem 3.** *The endemic equilibrium for the system is locally asymptotically stable if* $R_0 > 1$.

Proof. The Jacobian matrix at E^* is

$$J^* = \begin{bmatrix} -\alpha I^* - \mu & -\alpha S^* & 0 & 0 \\ \alpha I^* & \alpha S^* - (k_1 + k_2 + \mu + d_1) & 0 & 0 \\ 0 & k_1 & -(\gamma + \mu + d_2) & 0 \\ 0 & k_2 & \gamma & -\mu \end{bmatrix}.$$

In order to determine the local stability of the endemic equilibrium, it is sufficient to show that $\operatorname{Tr} J^* < 0$ and $\det J^* > 0$ [21]. Since

$$\alpha S^* - (k_1 + k_2 + \mu + d_1) = 0$$

(because $S^* = (k_1 + k_2 + \mu + d_1)/\alpha$), we get $\operatorname{Tr} J^* = -\alpha I^* - \mu < 0$ and

$$\det J^* = \alpha^2 S^* I^* = \left(\frac{N\alpha}{k_1 + k_2 + \mu + d_1} - \mu \right) (k_1 + k_2 + \mu + d_1) > 0$$

provided

$$\frac{N\alpha}{\mu(k_1 + k_2 + \mu + d_1)} > 1,$$

that is $R_0 > 1$. Hence the endemic equilibrium is locally stable if $R_0 > 1$. □

3.4.2. Global stability of the endemic equilibrium. **Theorem 4.** *The system (3.1)–(3.4) has no periodic orbits in* Ω.

Proof. We use Dulac's criterion. Let $X = (S, I, A, T)$ and consider the Dulac function $B = \frac{1}{IA}$. Then

$$B\frac{dS}{dt} = \frac{N}{IA} - \frac{\alpha S}{A} - \frac{\mu S}{IA},$$

$$B\frac{dI}{dt} = \frac{\alpha S}{A} - \frac{(k_1 + k_2 + \mu + d_1)}{A},$$

$$B\frac{dA}{dt} = \frac{k_1}{A} - \frac{(\gamma + \mu + d_2)}{I},$$

$$B\frac{dT}{dt} = \frac{k_2}{A} + \frac{\gamma}{I} - \frac{\mu T}{IA}.$$

Hence

$$\frac{\partial}{\partial S}\left(B\frac{dS}{dt}\right) + \frac{\partial}{\partial I}\left(B\frac{dI}{dt}\right) + \frac{\partial}{\partial A}\left(B\frac{dA}{dt}\right) + \frac{\partial}{\partial T}\left(B\frac{dT}{dt}\right) = -\frac{\alpha}{A} - \frac{\mu}{IA} - \frac{k_1}{A^2} - \frac{\mu}{IA} < 0.$$

Therefore, by Dulac's criterion there exists no periodic solution in Ω. By the Poincaré–Bendixson theorem, all solutions of (3.1)–(3.4) that remain in Ω approach an equilibrium. As a consequence, the endemic equilibrium E^* is stable if $R_0 > 1$, otherwise it is unstable. □

4. Sensitivity analysis

This section explores the results of a sensitivity analysis conducted on the threshold parameter R_0. The primary goal of the analysis is to identify key parameters that strongly influence R_0, making them essential targets for intervention strategies. Sensitivity indices are utilized to measure how R_0 responds to changes in specific parameters. In this study, the forward sensitivity index is calculated in the form of the ratio of the variable's relative change in R_0 to the relative change in the corresponding parameter, providing insights into the most influential factors affecting the system [22].

Mathematically, it is expressed as

$$\varphi_{P_i}^{R_0} = \frac{\partial R_0}{\partial P_i} \times \frac{P_i}{R_0},$$

where

$$R_0 = \frac{\alpha N}{\mu(k_1 + k_2 + \mu + d_1)}.$$

The R_0 elasticity indices are given by:

$$\varphi_\alpha = \frac{N}{\mu(k_1 + k_2 + \mu + d_1)} \times \frac{\mu(k_1 + k_2 + \mu + d_1)}{N} = 1,$$

$$\varphi_N = 1,$$

$$\varphi_\mu = -1 - \frac{\mu}{(k_1 + k_2 + \mu + d_1)},$$

$$\varphi_{k_1} = \frac{-k_1}{(k_1 + k_2 + \mu + d_1)},$$

$$\varphi_{k_2} = \frac{-k_2}{(k_1 + k_2 + \mu + d_1)},$$

$$\varphi_{d_1} = \frac{-d_1}{(k_1 + k_2 + \mu + d_1)}.$$

A positive sensitivity index of R_0 with respect to a model parameter indicates that any change in the parameter value directly influences the magnitude of R_0. Specifically, an increase in the parameter will result in a corresponding rise in R_0, while a decrease in the parameter will lead to a reduction in R_0. With the help of the graphs in Figs. 2–3 we can understand the sensitivity of parameters on the basic reproduction number.

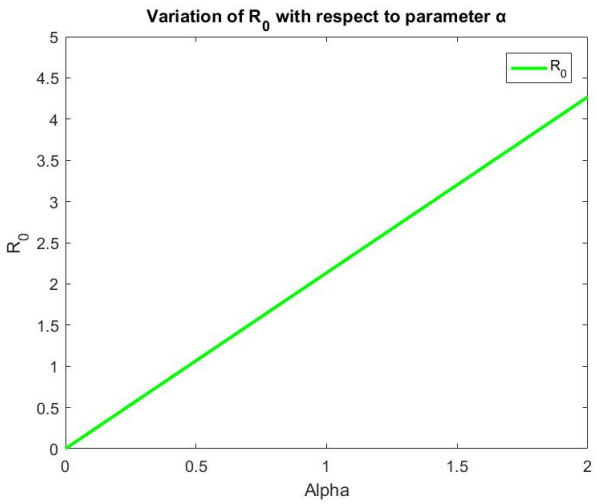

Figure 2: R_0 as a function of the parameter α.

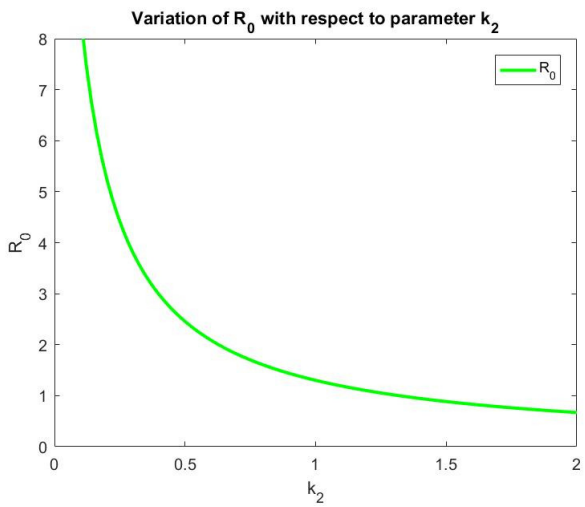

Figure 3: R_0 as a function of the parameter k_2.

From Fig. 2 we observe that in the SIAT model, the parameter α (the interaction parameter between susceptible and the HIV infected) has a positive sensitivity index, indicating that an increase in α leads to a rise in the basic reproduction number R_0, while a decrease in α results in a lower R_0. This suggests that α plays a significant role in driving the transmission dynamics of the infection. On the other hand, in Fig. 3 we find that the parameter k_2 (the parameter leaving HIV infected and entering the treated class) exhibits a negative sensitivity index, meaning that an increase in k_2 contributes to a reduction in R_0, whereas a decrease in k_2 leads to an increase in disease spread.

5. Optimal control

This section focuses on applying optimal control methods to effectively curb the transmission of HIV/AIDS. Our objective is to formulate and derive the necessary conditions that govern optimal intervention strategies within the framework of the HIV/AIDS SIAT model. Through this approach, we aim to enhance the understanding and implementation of targeted public health measures. To facilitate this, we introduce a time-dependent control variable $u(t)$, which represents various intervention strategies—such as treatment, vaccination, promotion of safe sexual practices and the use of uncontaminated syringes—applied at specific time points t. Thus, we have the following optimal control model:

$$\frac{dS}{dt} = N - [1 - u(t)]\,\alpha SI - \mu S, \tag{5.1}$$

$$\frac{dI}{dt} = [1 - u(t)]\,\alpha SI - (k_1 + k_2 + \mu + d_1)\,I, \tag{5.2}$$

$$\frac{dA}{dt} = k_1 I - (\gamma + \mu + d_2)A, \tag{5.3}$$

$$\frac{dT}{dt} = k_2 I + \gamma A - \mu T. \tag{5.4}$$

The objective functional is

$$\min_u J(u) = \min_u \int_0^{t_f} \left(c_1 I(t) + W_1 u^2(t)\right)\, dt,$$

where $0 \le u(t) \le 1$, $0 \le t \le t_f$, c_1 represents the positive constant weight that balances the individuals infected with HIV, and W_1 is a constant weight reflecting the significance of prevention control for HIV. The term $W_1 u^2(t)$ signifies the cost associated with the prevention control measures for HIV.

The Hamiltonian function is useful in epidemiological models for determining optimal intervention strategies (such as treatment, vaccination or awareness campaigns) that minimize the cost of infection or maximize health outcomes over time. It transforms the original control problem into a system of ODEs, allowing the use of Pontryagin's maximum principle [23].

The Hamiltonian function for the model is given by

$$\begin{aligned} H = c_1 I(t) + W_1 u^2(t) &+ \lambda_1 \left[N - (1 - u(t))\,\alpha SI - \mu S\right] \\ &+ \lambda_2 \left[(1 - u(t))\,\alpha SI - (k_1 + k_2 + \mu + d_1)\,I\right] \\ &+ \lambda_3 \left[k_1 I - (\gamma + \mu + d_2)A\right] + \lambda_4 \left[k_2 I + \gamma A - \mu T\right], \end{aligned} \tag{5.5}$$

where λ_i for $i = 1, 2, 3, 4$ are the adjoint variables corresponding to $S(t), I(t), A(t), T(t)$, respectively. Let $x_1 = S$, $x_2 = I$, $x_3 = A$, $x_4 = T$. Then

$$\frac{d\lambda_i}{dt} = -\frac{\partial H}{\partial x_i}, \qquad i = 1, 2, 3, 4.$$

We obtain

$$\frac{d\lambda_1}{dt} = -\frac{\partial H}{\partial S} = -\left\{-\lambda_1 (1 - u(t))\,\alpha I - \mu\lambda_1 + \lambda_2 (1 - u(t))\,\alpha I\right\},$$

$$\begin{aligned} \frac{d\lambda_2}{dt} = -\frac{\partial H}{\partial I} = -\Big\{ & c_1 - \lambda_1 (1 - u(t))\,\alpha S + \lambda_2 (1 - u(t))\,\alpha S \\ & - \lambda_2 (k_1 + k_2 + \mu + d_1) + \lambda_3 k_1 + \lambda_4 k_2 \Big\}, \end{aligned}$$

$$\frac{d\lambda_3}{dt} = -\frac{\partial H}{\partial A} = -\left\{-\lambda_3(\gamma + \mu + d_2) + \lambda_4\gamma\right\},$$

$$\frac{d\lambda_4}{dt} = -\frac{\partial H}{\partial T} = -\left(-\mu\lambda_4\right) = \mu\lambda_4.$$

The optimality condition for $0 \leq t \leq t_f$ is $\frac{\partial H}{\partial u} = 0$, that is

$$\frac{\partial H}{\partial u} = 2W_1 u(t) + \lambda_1 \alpha SI - \lambda_2 \alpha SI = 0,$$

whence

$$u(t) = \frac{\alpha SI\left(\lambda_1 - \lambda_2\right)}{2W_1}.$$

Since $0 \leq u(t) \leq 1$, we obtain the optimal control

$$u^*(t) = \min\left\{1, \max\left(0, \frac{\alpha SI\left(\lambda_1 - \lambda_2\right)}{2W_1}\right)\right\}.$$

Results of optimal control

If we simulate the optimal control in MATLAB, we obtain the following results.

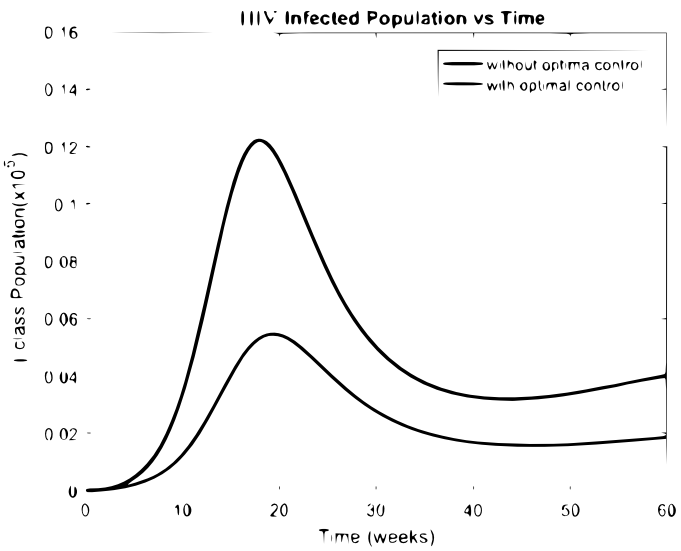

Figure 4: HIV infected class with and without optimal control.

Figs. 4–6 illustrate the outcome of implementing the optimal control strategy in the HIV/AIDS model. These figures provide a comparative analysis of the system's behavior with and without control interventions. In Fig. 4, the dynamics of the HIV-infected population is shown over time. Without optimal control, the number of HIV-infected individuals rises sharply and remains high, reflecting the uncontrolled spread of the disease. However, when optimal control measures are applied, a noticeable reduction in the infected population is observed.

Fig. 5 further supports this finding by presenting a consistent pattern of reduced AIDS infection levels under optimal control. The curve under the controlled scenario remains significantly lower compared to the uncontrolled case.

Fig. 6 depicts the behavior of the treated class over time. The graph shows that the number of treated individuals is lower under optimal control compared to the uncontrolled scenario. This is a positive outcome: because the infection rate is significantly reduced under control strategies, fewer individuals require treatment. Hence, the decline in the treated class corresponds to a reduced burden of disease in the population.

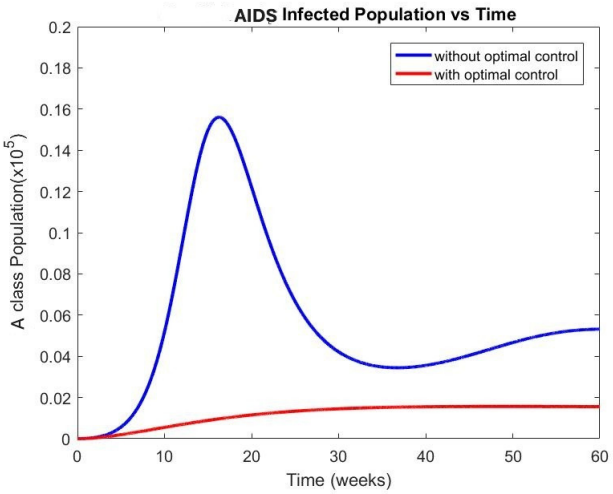

Figure 5: AIDS class with and without optimal control.

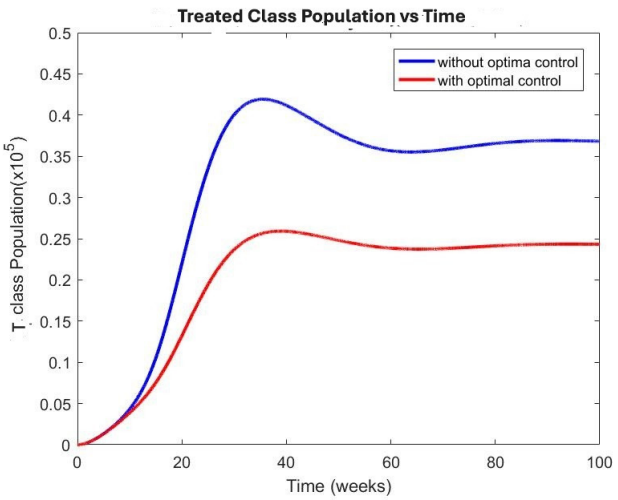

Figure 6: Treated class with and without optimal control.

Overall these graphs clearly demonstrate the effectiveness of the control strategy, leading to a substantial decline in the HIV-infected class over the simulation period.

6. Numerical simulation

We simulate the model by taking the parameter values from [24,25,26], given in Table 2.

We obtain the following graphical results.

Fig. 7 illustrates that, initially, the entire population belongs to the susceptible class. However, over time, this number declines as individuals transit into the HIV-infected class. The infected population rises, reaching a peak before gradually decreasing as individuals either progress to the AIDS stage or begin treatment. Similarly, the number of AIDS cases declines as more patients receive treatment. The treatment graph shows a steady increase, reflecting the growing number of individuals from both the HIV-infected and AIDS classes who have started undergoing treatment.

Fig. 8 depicts the influence of k_1 (the parameter leaving infected and entering into AIDS) on the AIDS

Table 2: Parameters and their values.

Parameters	Values	Source
α	0.7531	[24]
γ	0.0326	[26]
k_1	0.05945	[26]
k_2	0.0223	[25]
μ	0.0024	[25]
d_1	0.0015	[25]
d_2	0.00089	[25]

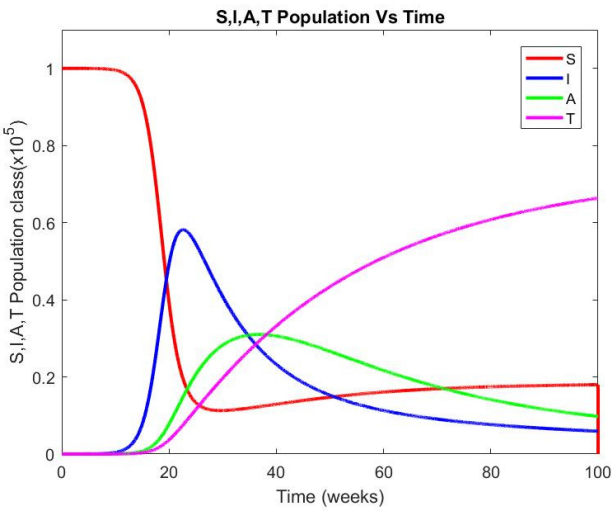

Figure 7: Time evolution of the SIAT model.

class. The graph indicates that a higher value of k_1 leads to a corresponding increase in the AIDS population, highlighting the direct relationship between the two.

Fig. 9 shows the effect of k_1 on the HIV-infected population. As k_1 increases, the infected population declines, suggesting that a higher transition rate from the infected stage to the AIDS stage reduces the number of individuals remaining in the infected class.

Fig. 10 shows the impact of k_2 (the rate of AIDS infected entering into the treated class) on the treated class. As k_2 increases it results in an increase in treated individuals.

Simulations for contour plots of the model

We obtain some contour plots for the basic reproduction number R_0 as a function of two different parameters chosen from Table 2.

From Fig. 11 we observe that R_0 increases with higher α (interaction/transmission rate) and decreases as k_1 (progression from HIV infection to AIDS) increases. This means that greater interaction rates lead to more secondary infections and thus amplify the epidemic potential. In contrast, faster progression from the infectious stage to AIDS shortens the average infectious period, thereby reducing the number of new infections. The highest R_0 values occur at high α combined with low k_1, representing the worst-case epidemic scenario.

From Fig. 12 we see that R_0 decreases as either k_1 (progression to AIDS) or k_2 (treatment initiation rate) increases. Both pathways remove individuals from the infectious pool— either by advancing them to AIDS (with lower assumed infectiousness) or by moving them into treatment (which suppresses viral

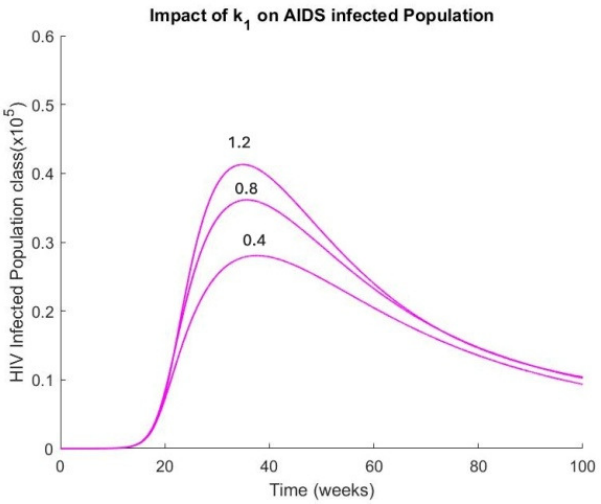

Figure 8: Impact of k_1 on the AIDS class.

load and reduces transmission). Thus, higher values of k_1 and k_2 act synergistically to lower transmission potential. The contour shows that even modest increases in k_2 can substantially reduce R_0, highlighting the critical role of timely treatment in epidemic control.

Finally, the relationship between α and d_1, demonstrated in Fig. 13, shows that although higher disease-induced mortality decreases R_0 by reducing the lifespan of infectious individuals, this reduction is achieved at the expense of higher mortality, underscoring that prevention measures aimed at reducing α are more effective and ethically appropriate.

Comparison of numerical methods

In the continuation we check the difference among three methods: Euler, Runge–Kutta 4th order and the Forward Difference method. The graphs obtained are given below.

Fig. 14 provides a detailed analysis of the influence of the parameter α (the rate of interaction between the susceptible and infected individuals) on the HIV-infected class, evaluated through three numerical methods: Euler, Runge–Kutta 4th order, and Forward Difference methods. The results demonstrate that an increase in α leads to a corresponding rise in the size of the infected class. Among the numerical methods applied, the Runge–Kutta 4th order method demonstrates superior performance due to its higher-order accuracy and greater numerical stability, making it a preferred choice for effectively capturing the system's dynamics.

Fig. 15 depicts the behavior of the AIDS class using the Runge–Kutta 4th order method and the Forward Difference method. Fig. 16 exhibits the HIV infected class dynamics using Runge–Kutta 4th order and Forward Difference methods. In Figs. 15 and 16, we observe that initially the absolute value disparities are minimal. However, as the number of iterations increases, so do the absolute value discrepancies, which eventually peak and then decline.

Fig. 17 displays the errors obtained in the numerical values calculated by both methods. The error graph shows that the Runge–Kutta 4th order method maintains significantly lower deviations in the infected population over time, whereas the Forward Difference method accumulates noticeable error due to its lower-order approximation. The numerical errors in the $I(t)$ class given by both methods are summarized in Table 3.

This emphasizes the accuracy of the Runge–Kutta 4th order method in precisely capturing the dynamics of infectious disease spread.

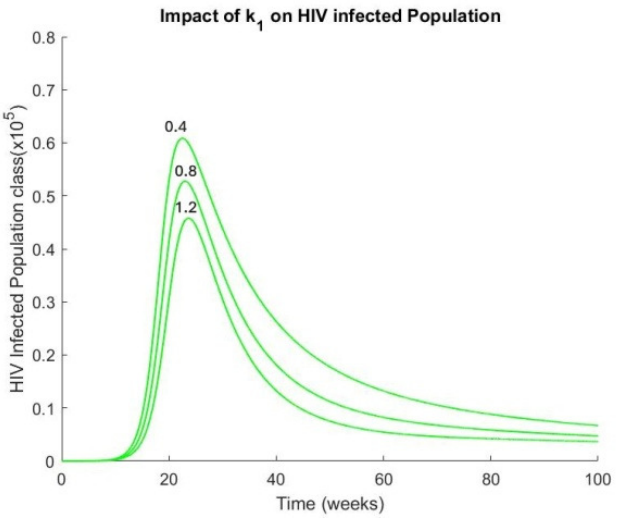

Figure 9: Impact of k_1 on the HIV infected class.

Table 3: Methods and errors.

Method	**Error**
Forward Difference	0.0162
Runge–Kutta 4th order	0.0000

7. Conclusion

In this study, we developed a nonlinear SIAT model to capture the transmission dynamics of HIV/AIDS, categorizing the population into susceptible, infected, AIDS, and treated classes. A key novelty of our work lies in combining rigorous analytical techniques with a systematic comparison of three numerical schemes—Euler, Runge–Kutta (4th order), and Forward Difference methods—within the context of HIV/AIDS modeling. Our results demonstrate that while all methods are capable of reproducing the theoretical behavior, the Runge–Kutta method consistently yields superior accuracy and stability, establishing it as a benchmark for future computational epidemiology studies.

Another significant finding is the identification of the interaction rate (α) and transmission parameters (k_1, k_2) as dominant drivers of epidemic progression. Sensitivity analysis not only highlights these parameters but also provides actionable insights for prioritizing public health interventions. Furthermore, by integrating optimal control theory, we show how preventive and treatment-based strategies—such as safe practices and consistent ART adherence—can be systematically optimized to reduce infections and delay progression to AIDS.

Collectively, this research contributes to mathematical epidemiology in two novel ways: (i) by establishing a comparative framework for evaluating numerical methods in HIV/AIDS dynamics, and (ii) by linking sensitivity-guided parameter prioritization with optimal control to inform effective intervention strategies. These findings open pathways for extending the model to include co-infections, treatment resistance, and heterogeneous populations, thereby enhancing its real-world applicability.

Statements and Declarations

All of the authors have equally contributed in writing this paper. This research did not receive any specific grant from funding agencies in the public, commercial, or not-for-profit sectors. The authors declare no conflict of interest.

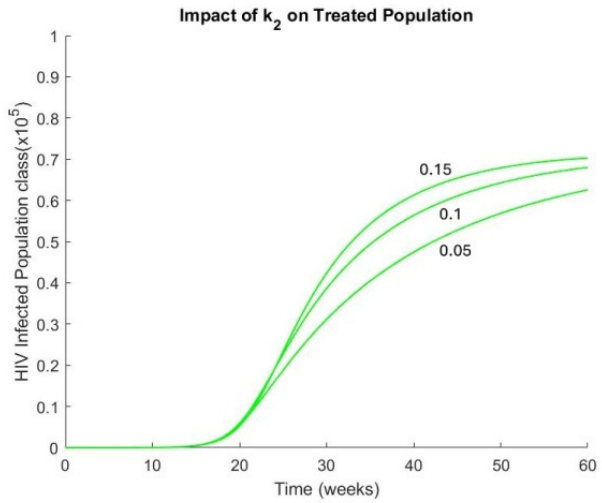

Figure 10: Impact of k_2 on the treated class.

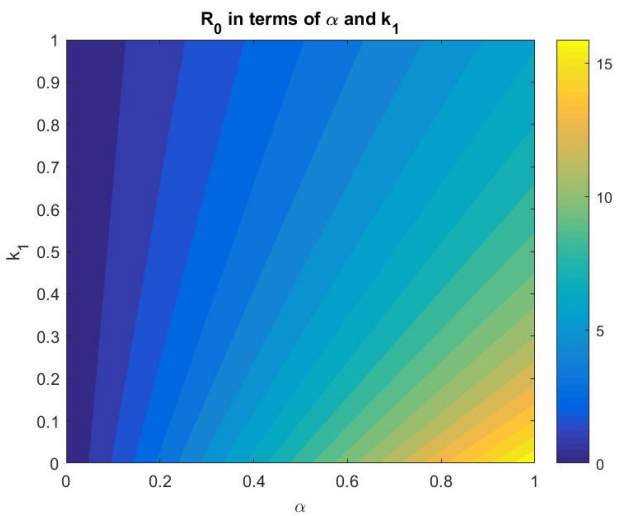

Figure 11: Impact of α and k_1 on R_0.

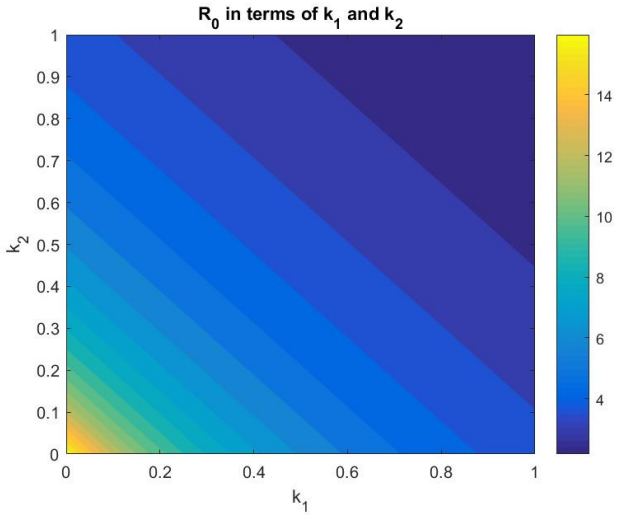

Figure 12: Impact of k_1 and k_2 on R_0.

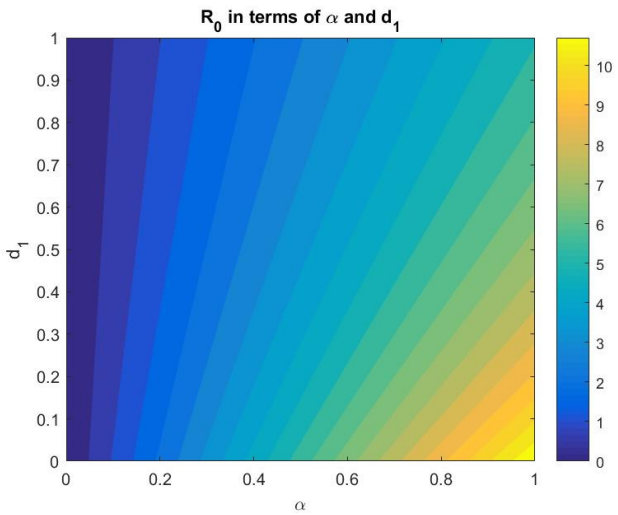

Figure 13: Impact of α and d_1 on R_0.

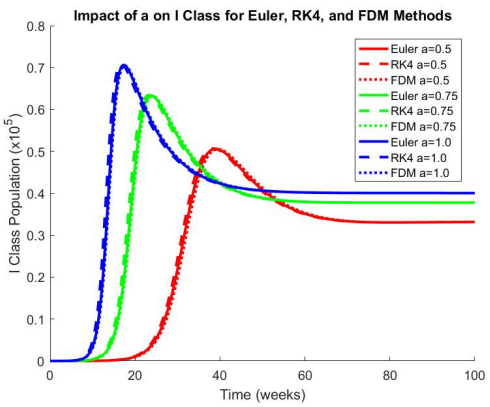

Figure 14: Impact of α on the HIV infected class by all three methods.

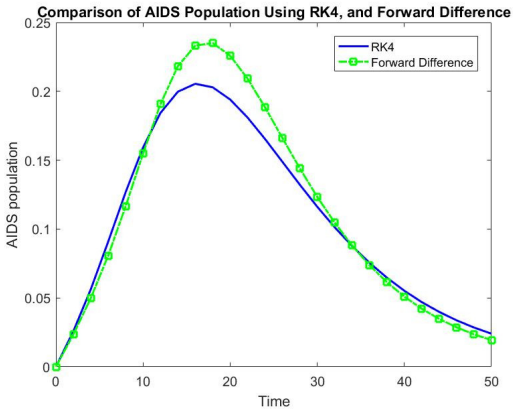

Figure 15: AIDS class using RK4 and Forward Difference method.

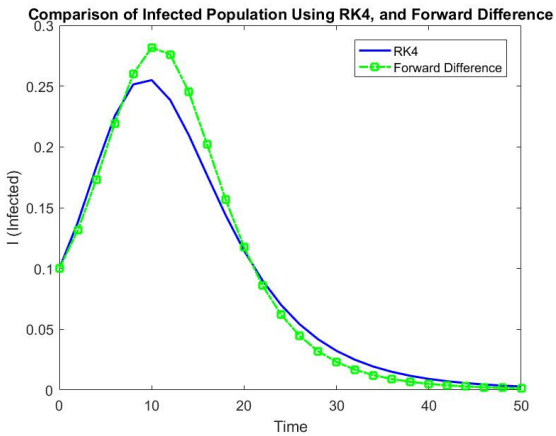

Figure 16: HIV infected class by RK4 and Forward Difference method.

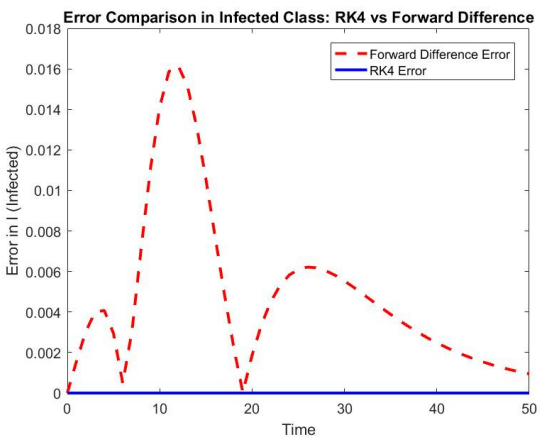

Figure 17: Error comparison in infected class by RK4 and Forward Difference method.

References

1. "HIV." Accessed: Jan. 15, 2025. Available at `https://www.who.int/data/gho/data/themes/hiv-aids`.
2. N. K. Jothi, V. V, S. K. Dayalan, J. Giri, W. A. Hatamleh, and H. Panchal, Dynamic interactions of HSV-2 and HIV/AIDS: A mathematical modeling approach, *AIP Advances* **14** (2024), 035326.
3. S. Olaniyi, J. O. Olayiwola, O. S. Obabiyi, R. S. Lebelo, and S. F. Abimbade, Mathematical Analysis of Non-Autonomous HIV/AIDS Transmission Dynamics with Efficient and Cost-Effective Intervention Strategies, *Contemporary Mathematics* (2025), 1380–1400.
4. L. Rong, Z. Feng, and A. S. Perelson, Mathematical Modeling of HIV-1 Infection and Drug Therapy, in *Mathematical Modelling of Biosystems*, Springer, Berlin, 2008, pp. 87–131.
5. T. K. Ayele, E. F. Doungmo Goufo, and S. Mugisha, Mathematical modeling of HIV/AIDS with optimal control: A case study in Ethiopia, *Results in Physics* **26** (2021), 104263.
6. R. M. May and R. M. Anderson, Transmission dynamics of HIV infection, *Nature* **326** (1987), 137–142.
7. D. N. Burns et al., Toward an Endgame: Finding and Engaging People Unaware of Their HIV-1 Infection in Treatment and Prevention, *AIDS Res. Hum. Retroviruses* **30** (2014), 217–224.
8. S. M. Blower, H. B. Gershengorn, and R. M. Grant, A Tale of Two Futures: HIV and Antiretroviral Therapy in San Francisco, *Science* **287** (2000), 650–654.
9. S. Waziri, S. Massawe, and O. Makinde, Mathematical Modelling of HIV/AIDS Dynamics with Treatment and Vertical Transmission, *Applied Mathematics* **2** (2012), 77–89.
10. M. Shen, Y. Xiao, L. Rong, L. A. Meyers, and S. E. Bellan, Early antiretroviral therapy and potent second-line drugs could decrease HIV incidence of drug resistance, *Proc. Biol. Sci.* **284** (2017), 20170525.
11. D. Fajardo-Ortiz et al., The emergence and evolution of the research fronts in HIV/AIDS research, *PLoS One* **12** (2017), e0178293.
12. Attaullah and M. Sohaib, Mathematical modeling and numerical simulation of HIV infection model, *Results in Applied Mathematics* **7** (2020), 100118.
13. H. Sun et al., Dynamics of HIV transmission among men who have sex with men in Taiwan: a mathematical modeling study, *BMC Public Health* **24** (2024), 3063.
14. A. H. Morani, M. M. Saeed, M. Aslam, A. Mehmoud, A. Shokri, and H. Mukalazi, Local and global stability analysis of HIV/AIDS by using a nonstandard finite difference scheme, *Sci. Rep.* **15** (2025), 4502.
15. R. Ashgi et al., Comparison of Numerical Simulation of Epidemiological Model between Euler Method with 4th Order Runge Kutta Method, *Int. J. Global Operations Research* **2** (2020), 67.
16. A. M., G. C., and Q. M. Al-Mdallal, Mathematical modeling and simulation of SEIR model for COVID-19 outbreak: A case study of Trivandrum, *Front. Appl. Math. Stat.* **9** (2023), 1124897.
17. U. D. Ghoshna, *Numerical Methods*, online notes, available at `https://udghoshna.wordpress.com/wp-content/uploads/2013/06/numerical-methods.pdf`.
18. G. Macdonald, The analysis of equilibrium in malaria, *Trop. Dis. Bull.* **49** (1952), 813–829.
19. S. W. Teklu, T. T. Guya, B. S. Kotola, and T. S. Lachamo, Analyses of an age structure HIV/AIDS compartmental model with optimal control theory, *Sci. Rep.* **15** (2025), 5491.
20. E. J. Routh, *A Treatise on the Stability of a Given State of Motion, Particularly Steady Motion*, Macmillan, 1877.
21. A. Hassen, B. Carpentieri, K. G. Mekonen, L. L. Obsu, and S. F. Balcha, Mathematical Modeling and Analysis of TB and COVID-19 Coinfection, *J. Appl. Math.* (2022), Art. ID 2449710.
22. A. El Bhih, Y. Benfatah, H. Hassouni, O. Balatif, and M. Rachik, Mathematical modeling, sensitivity analysis, and optimal control of students awareness in mathematics education, *Partial Differential Equations in Applied Mathematics* **11** (2024), 100795.
23. A. Di Liddo, Optimal Control and Treatment of Infectious Diseases. The Case of Huge Treatment Costs, *Mathematics* **4** (2016), 2.
24. N. Kaur, M. Ghosh, and S. S. Bhatia, Mathematical Analysis of the Transmission Dynamics of HIV/AIDS: Role of Female Sex Workers, *Appl. Math. Inf. Sci.* **8** (2014), 2491–2501.
25. S. Saravanakumar, A. Eswari, L. Rajendran, and M. Abukhaled, A Mathematical Model of Risk Factors in HIV/AIDS Transmission Dynamics: Observational Study of Female Sexual Network in India, *Appl. Math. Inf. Sci.* **14** (2020), 967–976.
26. C. C. Espitia, M. A. Botina, M. A. Solarte, I. Hernandez, R. A. Riascos, and J. F. Meyer, Mathematical Model of HIV/AIDS Considering Sexual Preferences Under Antiretroviral Therapy, a Case Study in San Juan de Pasto, Colombia, *J. Comput. Biol.* **29** (2022), 483–493.

Kshama Jain,
Department of Mathematics,
Dayananda Sagar University,

India.
E-mail address: goyal.kshama23@gmail.com

and

Anuradha Bhattacharjee,
Department of Science and Humanities,
PES University,
India.
E-mail address: bhattacharjee.anuradha@gmail.com

and

Srikumar K.,
Department of Mathematics,
Dayananda Sagar University,
India.
E-mail address: srimalatkar@gmail.com